

# Spatio-Temporal Shifting to Reduce Carbon, Water, and Land Use Footprints of Cloud Workloads

Giulio Attenni<sup>a</sup>, Youssef Moawad<sup>b</sup>, Novella Bartolini<sup>a</sup>, Lauritz Thamsen<sup>b</sup>

<sup>a</sup>*"La Sapienza" University of Rome, Department of Computer Science, Rome, Italy*

<sup>b</sup>*University of Glasgow, School of Computing Science, Glasgow, United Kingdom*

---

## Abstract

In this paper, we investigate the potential of spatial and temporal cloud workload shifting to reduce carbon, water, and land use footprints. Specifically, we perform a simulation study leveraging publicly available data on the cloud infrastructure of major providers (AWS and Azure) as well as real-world workload traces (big data analytics and FaaS) and grid mix data to consider two different scenarios. Our simulation results indicate that spatial shifting can substantially lower carbon, water, and land use footprints. In the FaaS applications, shifting the spatiotemporal workload achieves carbon savings of up to 85%, water savings of around 50%, and reductions in land use of up to 45%, all while optimizing for the respective factors. Mixed optimization yields results comparable to those of land use alone. For big data workloads, spatiotemporal shifting delivers reductions of up to 45% in carbon emissions, 40% in water consumption, and nearly 40% in land use when optimized for the respective factors. Temporal shifting also decreases the footprint, though to a lesser extent. When applied together, the two strategies yield the greatest overall reduction, driven mainly by spatial shifting with temporal adjustments providing an additional, incremental benefit. Sensitivity analysis demonstrates that such shifting is robust to prediction errors in grid mix data and to variations across different seasons.

*Keywords:* Carbon-aware computing, sustainable computing, cloud computing, big data, serverless computing

---

## 1. Introduction

The Information and Communication Technology (ICT) sector is estimated to be responsible for 1.8%–2.8% of global GHG emissions [1] and this share is expected to rise in the future [2]. In particular, data centers have become one of the most energy-intensive infrastructures, with their electricity consumption projected to reach around 945 TWh globally by 2030 [3]. This growth is driven by data-intensive applications and services, including artificial intelligence and big data analytics.

The sustainability of cloud computing has been studied, with a primary focus on reducing carbon emissions. A wide body of work investigates carbon-aware scheduling and orchestration, exploiting spatial [4, 5, 6, 7, 8], temporal [9, 10, 11], and spatio-temporal [12, 13, 14, 15, 16] shifting of workloads to align demand with low-carbon electricity availability.

Recently, studies have started to address the significant environmental impacts of cloud computing beyond carbon emissions. In particular, the impacts of water consumption have seen attention [17, 18]. Additionally, large-scale land use, as associated with data center construction, can lead to habitat disruption and biodiversity loss [19]. These factors underscore the need for a multi-dimensional approach to evaluating and optimizing the environmental footprint

of cloud computing. To the best of our knowledge, land use has not been systematically integrated into sustainability-aware scheduling of cloud workloads before. We, therefore, address this gap by introducing *Land Usage Effectiveness (LUE)* as a metric and incorporating it into the multi-dimensional optimization of workload placement.

In this paper, we investigate the spatial and temporal shifting of cloud workloads as strategies to reduce carbon, water, and land use footprints. We conduct an extensive simulation study using real-world data from major public cloud providers (Azure and AWS) and representative cloud workloads (FaaS and big data analytics), demonstrating the potential of multi-dimensional sustainability-aware scheduling.

In summary, our main contributions are:

- We propose a holistic formulation for workload scheduling that optimizes carbon, water, and land use impacts, leveraging temporal and spatial cloud workload shifting
- We provide a systematic evaluation based on real-world workload traces and grid mix data, quantifying trade-offs under spatial, temporal, and spatio-temporal shifting scenarios. Moreover, we conduct sensitivity studies on workload flexibility, grid mix prediction errors, and seasonal variations.

- We release all code and data from this study to support transparency, reproducibility, and further research <sup>1</sup>.

The rest of the paper is organized as follows. Section 2 provides background on data center environmental impacts. Section 3 presents our system model and problem formulation. It also describes our methodology, including the proposed optimization algorithms. Section 5 presents our simulation setup, including a detailed description of the scenario characteristics such as workload types, data center specifications, and grid datasets. Section 6 presents the results of our empirical evaluation and discusses our findings as well as threats to validity. Section 8 reviews related work. Finally, Section 9 concludes the paper and outlines directions for future research.

## 2. Background - Data Center Impacts

Data centers rank among the world’s most energy intensive facilities, consuming vast quantities of electricity to run servers, cooling infrastructure, and backup power systems. This substantial energy demand translates into considerable greenhouse gas (GHG) emissions, particularly in regions that rely heavily on fossil fuels for electricity generation. As a result, the environmental footprint of any given data center is closely linked to the composition of its local power grid.

The energy mix influences the *Carbon Intensity (CI)*, which measures the greenhouse gas emissions per unit of electricity consumed (typically expressed in gCO<sub>2</sub>e/kWh); the *Energy Water Intensity Factor (EWIF)*, which captures the amount of water withdrawn or consumed during electricity generation (measured in liters/kWh), which varies with the cooling technologies; and the *Energy Land Intensity Factor (ELIF)*, which quantifies the land use required for producing electricity (expressed in m<sub>2</sub>/kWh). Example estimates of these intensities are reported in [20, 21, 22]. These are also the main sources used in our experiments (see Table 5.1), and in the discussion section, we will analyze how these coefficients relate to each other.

The efficiency of data center operations also depends on the infrastructure and technologies used. The *Power Usage Effectiveness (PUE)* is defined as the ratio of the total energy consumed by a datacenter facility to the energy consumed by its IT equipment [23]. A PUE of 1.0 indicates ideal efficiency, where all energy is used exclusively for computation.

Moreover, the efficiency of cooling systems, which are essential to prevent overheating of servers, can significantly affect water usage. The choice of cooling technology (e.g., air cooling vs. liquid cooling) can lead to different water consumption. The *Water Usage Effectiveness (WUE)* measures the water consumption of a data center relative

to its IT energy usage, typically expressed in liters of water per kilowatt-hour (l/kWh) [24].

Finally, since these infrastructures occupy a significant amount of land, the *Land Usage Effectiveness (LUE)* [25] should also be considered. To the best of our knowledge, this metric has not been standardized, and it has not been used previously. Similar to PUE and WUE, the LUE metric aims to quantify the physical land footprint of data centers in relation to IT energy consumption, capturing the spatial resource requirements of large-scale compute infrastructure. Thus, for the scope of our work, we define it as the ratio of the total land occupied by the data center property and the IT energy consumption, and it is, therefore, expressed in square meters per kilowatt-hour (m<sup>2</sup>/kWh).

The carbon associated with the extraction, processing, and transportation of construction materials, as well as with the production of IT equipment (known as embodied carbon) accounts for a share of the total carbon footprint of a data center. However, in this work, we consider only the share of operational carbon emissions of the workloads.

## 3. Problem Statement

Before presenting the methodology of our study, we first formalize the problem in this section.

### 3.1. System Model

First of all, let us consider the temporal horizon  $H$ , and let us discretize the time. Thus, let us define  $\mathcal{T} = [t_0, t_0 + \delta_t, t_0 + 2\delta_t, \dots, H]$ , as the set of time steps. Let us also define  $\mathcal{D}$  as the set of regions/data centers, and consider a data center  $d$  and a time  $t$ . To evaluate its impact accounting for multiple factors (i.e., carbon, water, and land use), we define its sustainability profile as follows:

$$\forall t \in \mathcal{T}, d \in \mathcal{D} \quad \mathbf{p}_d(t) = \begin{pmatrix} C_d(t) \\ W_d(t) \\ L_d(t) \end{pmatrix} \quad (1)$$

where:

- $C_d(t)$  is the predicted carbon intensity of data center  $d$  from time  $t$  to time  $t + \delta_t$  and it is defined as

$$CI_{G_d}^e(t) \times PUE_d \quad (2)$$

It is measured in  $\frac{gCO_2}{kWh}$  and represents the carbon emitted per kWh consumed. We consider the carbon intensity prediction of the regional grid of data center  $d$  at time  $t$ , namely  $CI_{G_d}^e(t)$ , where  $e$  is the predictive model and  $G_d$  is the grid. This intensity is multiplied by the Power Usage Effectiveness of the data center,  $PUE_d$ , to account for the overall energy usage of a data center for each kWh of computation.

<sup>1</sup><https://github.com/GlasgowC31ab/CaWaLand>

<i>Symbol</i>	<i>Description</i>
$t_0, H, \delta_t, \mathcal{T}$	period start, end, step duration and set of steps
$d, \mathcal{D}$	region/data center and set of regions/data centers
$PUE_d$	region PUE
$WUE_d$	region WUE
$LUE_d$	region LUE
$A_d$	region land occupation area
$IT_d$	region IT energy usage
$\mathcal{C}_d(t)$	region carbon footprint
$\mathcal{W}_d(t)$	region water footprint
$\mathcal{L}_d(t)$	region land footprint
$CI_{G_d}^e(t)$	region Energy Carbon Intensity prediction
$EWIF_{G_d}^e(t)$	region Energy Water Intensity Factor prediction
$ELIF_{G_d}^e(t)$	region Energy Land Intensity Factor prediction
$p_d(t)$	data center footprint profile at time t
$p_d^{norm}(t)$	normalized data center footprint profile at time t
$p_{global}^{norm}(t)$	global footprint profile
$v, \mathcal{V}$	VM instance and set of VM instances
$P_{v,j}$	VM $v$ power draw for job $j$
$B_v$	VM's network bandwidth
$j, \mathcal{J}$	job and set of jobs
$o_j, a_j, t_j$	job's arrival location and arrival and deadline time
$s_j, \mathcal{D}[j]$	job's data size and region availability
$v_j, n_j$	job's configuration (VM instance and nr. of nodes)
$r_j$	job's expected runtime
$C(j, d, t)$	scheduling footprints
$M(j, d, t)$	migration/data transfer footprints
$NEI$	Network Energy Intensity
$L(j, d)$	migration/data transfer latency
$E(j, d, t)$	execution footprint

Table 1: Notations

- $\mathcal{W}_d(t)$  is the predicted water intensity and it is defined as

$$WUE_d + EWIF_{G_d}^e(t) \times PUE_d \quad (3)$$

We compute the water intensity considering both the on-site and grid contributions. It is measured in  $\frac{l}{kWh}$  and represents the water consumed per kWh, considering the average Energy Water Intensity Factor prediction of the regional grid,  $EWIF_{G_d}^e(t)$ , and the Water Usage Effectiveness of the data center,  $WUE_d$ .

- $\mathcal{L}_d(t)$  is the predicted land use intensity and it is defined as

$$LUE_d + ELIF_{G_d}^e(t) \times PUE_d \quad (4)$$

Similarly to the water intensity, we consider both on-site and grid contributions. It is measured in  $\frac{m^2}{kWh}$ , and it is the amount of land used per kWh considering the Energy Land Intensity Factor prediction of the regional grid at time  $t$ ,  $ELIF_{G_d}^e(t)$ , and the Land Usage Effectiveness, defined as  $LUE_d = \frac{A_d}{P_d^{IT}}$ . In this formula,  $A_d$  is the total area of land occupied by the data center property and  $P_d^{IT}$  is the energy used to power the IT equipment.

The aforementioned energy intensity factors of the electric grid intensity depends on the energy mix, which is both time and space-dependent. Thus, let us define  $S$  as the list of sources in the energy mix, namely  $\{Solar, Wind, Hydro, Geothermal, Biomass, Nuclear, Coal, Gas, Oil, Unknown\}$ , and let  $MIX_{G_d,s}^e(t)$  be the share of source  $s \in S$  in the mix prediction of  $G_d$ . Thus, we can define the energy intensity factors as:

- $CI_{G_d}^e(t) = \sum_{s \in S} MIX_{G_d,s}^e(t) \times CI_s$
- $EWIF_{G_d}^e(t) = \sum_{s \in S} MIX_{G_d,s}^e(t) \times EWIF_s$
- $ELIF_{G_d}^e(t) = \sum_{s \in S} MIX_{G_d,s}^e(t) \times ELIF_s$

where  $CI_s$ ,  $EWIF_s$  and  $ELIF_s$  are specified in table 5.1.

Moreover, let us define  $\mathcal{V}$  as the set of virtual machine instances, for each  $v \in \mathcal{V}$  it is known the power draw in relation to a certain job  $j \in \mathcal{J}$ ,  $P_v$  defined according to the Cloud Carbon Footprint methodology<sup>2</sup>.

Finally, let us also define the set of job requests  $J$ . For each request  $j \in J$  it is known: the arrival/origin region/location  $o_j \in \mathcal{D}$ , the regions in which data is available  $\mathcal{D}[j] \subseteq \mathcal{D}$ , data size  $s_j \in \mathbb{N}$ , number of nodes  $n_j \in \mathbb{N}$ , the expected utilization  $u_j \in \mathbb{N}$ , the VM instance  $v_j \in \mathcal{V}$ , the expected runtime  $r_j \in \mathbb{Z}$ , the arrival time  $a_j \in \mathcal{T}$ , and the deadline  $t_j \in \mathcal{T}$ .

We aim to optimize footprints associated with the job requests scheduling, considering both data migration and execution, by leveraging spatio-temporal shifting approaches.

<sup>2</sup><https://www.cloudcarbonfootprint.org/docs/methodology>

## 4. Methodology

In this section, we present our methodology. We define an evaluation method for the footprints associated with a job request. Then we present the scheduling methods considered in our evaluation. Finally, we present our experiment design.

### 4.1. Evaluating Environmental Footprints

Firstly, we need a methodology to evaluate the footprints of executing a request in a certain region at a certain time. Let us consider that we want to predict the associated footprint of computing a job request  $j$  in region/data center  $d$  at time  $t$ . If the data related to the request is not available in  $d$ , data migration is required, and it is necessary to account for its environmental impact.

To account for migration footprint overhead, data transmission energy is estimated as follows:

$$M(j, d, t) = \begin{cases} s_j \times NEI & \text{if } d \notin \mathcal{D}[j] \\ 0 & \text{otherwise} \end{cases} \quad (5)$$

where  $NEI$  kWh/GB is the Network Energy Intensity, as proposed in [26].

To calculate the execution footprint, we need to know when executions start. We assume that if data is not migrated, the execution start would be at the arrival time, since the scheduling execution time is negligible. If the data needs to be migrated, we need to compute the data migration latency as follows:

$$L(j, d) = \begin{cases} \frac{s_j}{B_{v_j}} & \text{if } d \notin \mathcal{D}[j] \\ 0 & \text{otherwise} \end{cases} \quad (6)$$

To account for the execution footprint, we define

$$E(j, d, t) = \int_{t+L(j,d)}^{t+L(j,d)+r_j} P_{v,j} \cdot \mathbf{p}_d^{norm}(\tau) d\tau \quad (7)$$

where  $\mathbf{p}_d^{norm}(t) \in \mathbb{R}^3$  is the normalized profile vector of region  $d$  for carbon, water, and land use. We define the normalization operator applied component-wise.

$$\mathcal{N}(\mathbf{p}_d(t)) = \frac{\mathbf{x} - \min_{d,t} \mathbf{p}_d(t)}{\max_{d,t} \mathbf{p}_d(t) - \min_{d,t} \mathbf{p}_d(t)}$$

Thus, the regional normalized profile is  $\mathbf{p}_d^{norm}(t) = \mathcal{N}(\mathbf{p}_d(t))$ . We shall consider global intensities to account for migration footprint, and we define them as the normalized (over time) average intensities, namely:  $\mathbf{p}_{global}^{norm}(t) = \mathcal{N}(\text{avg}_d \mathbf{p}_d(t))$ . Finally, we can compute the overall environmental cost of scheduling the job.

$$C(j, d, t) = (E(j, d, t) + M(j, d, t) \times \mathbf{p}_{global}^{norm}(t)) \times \theta \quad (8)$$

where  $\theta$  is the weight vector to linearly combine the three impact factors, namely:  $\theta = (w_C \quad w_W \quad w_L)$ .

### 4.2. Scheduling Methods

We consider the following shifting methods:

- *Spatial Shifting*: jobs should be executed where their overall impact is minimized (considering data migration when required).

$$d^*, t^* = \text{argmin}_{d \in \mathcal{D}} C(j, d, a_j), a_j \quad (9)$$

- *Temporal Shifting*: jobs should be executed when their overall impact is minimized.

$$d^*, t^* = o_j, \text{argmin}_{t \in [a_j, t_j - r_j]} C(j, o_j, t) \quad (10)$$

- *Spatio-Temporal Shifting*: optimize both when and where the jobs' overall impact is minimized.

$$d^*, t^* = \text{argmin}_{d \in \mathcal{D}, t \in [a_j, t_j - (r_j + L(j,d))]} C(j, d, t) \quad (11)$$

For methods including spatial shifting, we assume that once data is transferred to another region, the origin location persistently stores the data. We do this to assume that for periodic jobs, data will be available in multiple regions without transferring it multiple times. As a baseline, we consider a method in which jobs are executed where the request originates, namely the *Local* baseline:

$$d^*, t^* = o_j, a_j \quad (12)$$

### 4.3. Experiment Design

In this work, we focus on two types of workloads. We have selected two workloads: a user-facing, latency-sensitive workload (FaaS) and a delay-tolerant batch processing workload (big data). For each workload type, we considered real traces and derived two real-world scenarios to simulate their scheduling and execution.

*Aim.* The aim of our experiments is to investigate environmentally conscious cloud workload shifting through realistic simulations, not to compare real-world providers. Our results may not accurately reflect the impact of real-world workloads on AWS or Azure data centers, because, although our scenarios are inspired by published data where possible, assumptions and approximations are made where exact data was not available.

*Simulation Overview.* We implemented the discrete event simulation detailed in Algorithm 1. At each time step, we update the sustainability profiles of data centers and new job requests ready to be scheduled. Then each job can be scheduled according to the shifting approach previously defined. Finally, since we assume that once data is transmitted to a region, it is persistently stored there, the data availability set of the job is updated for future scheduling.

---

**Algorithm 1** Simulation Procedure

---

```
1: Input:  $\mathcal{D}$  data centers, scheduling_method()  $\in$ 
   {eq.(9), eq.(10), eq.(11), eq.(12)}
2: for  $t \in \mathcal{T}$  do
3:   Get sustainability profiles  $p_d(t)$  for each  $d \in \mathcal{D}$ 
4:   Get jobs ready to be scheduled at time  $t$ ,  $J(t)$ .
5:   for  $j$  in  $J(t)$  parallel do
6:      $d^*, t^* = \text{scheduling\_method}()$ 
7:     if scheduling_method()  $\in$  {eq.(9), eq.(11)}
       then
8:        $\mathcal{D}[j] = \mathcal{D}[j] \cup \{d^*\}$ 
9:     end if
10:  end for
11: end for
12: Output: Final schedule over horizon  $H$ 
```

---

*Scenario 1 - Azure and FaaS.* The first scenario is based on Azure regions and a FaaS workload. The regions selected for this scenario are "swedencentral", "southcentralus", "centralus", and "eastus". Table 4.3 reports regions' characteristics. PUE and WUE values were taken from Azure issued sustainability reports. The land occupation data stems from online reports. As for the workload, we chose the 2019 Azure Functions dataset. For the data sources see Appendix A. The source data is composed of two sets of daily CSV files: one detailing per-minute invocation counts for each function, and another providing daily summary statistics of function execution times, including averages and key percentiles (0th, 1st, 25th, 50th, 75th, 99th, and 100th). We utilised the first seven days of this dataset to synthesise 100,000 requests of function execution a day. The selection of a function for each request was probabilistic and weighted by the function's total daily invocation count, such that more frequently invoked functions appeared more often in the trace, mirroring real-world usage patterns.

Upon selecting a function, we sampled a synthetic runtime by performing linear interpolation on its known daily execution time percentiles. The arrival time for the request, resolved to the minute-of-day, was similarly sampled from the function's empirical per-minute invocation distribution. Finally, each request was assigned a data center location from a predefined set. A single virtual machine configuration (2 vCPU and 4 GB of RAM) is considered for this scenario, as specified in the paper [27].

For this scenario, we compare only the *Local* baseline (L) and the *Spatial Shifting* (SP) approach. That is, we assume that the functions are tolerant to the latency required to change regions but not to be delayed in time. For this reason, we exclude *Temporal Shifting* (T) and *Spatio-temporal Shifting* (STP) scheduling methods. Thus, there are no deadlines for this scenario.

*Scenario 2 - AWS and Big Data.* The second scenario is based on AWS and Big Data workloads. The regions selected for this scenario are: "us-east-1", "us-west-1", "eu-

<i>Region</i>	<i>Location</i>	<i>PUE</i>	<i>WUE</i>	<i>Land Occupation (sqm)</i>
swedencentral	Sweden	1.172	0.16	1300000
southcentralus	Texas	1.307	1.82	43664
centralus	Iowa	1.16	0.19	37904
eastus2	Virginia	1.144	0.17	102193

Table 2: Azure data by Region for Scenario 1.

central-1", "eu-west-2", and "eu-north-1". Table 4.3 reports regions' characteristics. PUEs and WUEs values were taken from AWS website (see Appendix A)

The land occupation data is estimated based on the 10-k form released by AWS in 2024 (see Appendix A), in which it is stated that more than 450,000 sqmt were owned/rented by AWS for data centers. The estimation is also based on declared availability zones for each region. Namely, the estimated land occupation for a given region is calculated by taking the number of availability zones (AZs) in that region, dividing it by the total number of AZs (117), and then multiplying by the total land occupation of all data centers.

As for the workload, we synthetically generate requests from available experimental Spark traces (see Appendix A). We randomly generated 50k requests over a week. For the arrival pattern, we generated 50% of requests as periodic (in line with literature analysis: about 43% [28], about 60% [29]) and the rest as ad-hoc jobs. We generate synthetic requests for each day of the selected week. The arrival of ad-hoc jobs follows a Poisson distribution with  $\lambda = \text{target}_{np} / n_{days} * \text{minutesperday} \approx 2.5$ . The periodic jobs' first instance arrival time is randomly picked within the first 12 hours, and their periodicity is set uniformly at random among  $\{2, 4, 8, 12\}$  hours. For each request, the origin location is picked uniformly at random from the regions considered for this scenario. The number of nodes, the VM instance, and the expected runtime are the ones reported in the traces. Table 4.3 summarizes the VM instances considered in our experiments, and their specifications are set accordingly (memory, cpu, and bandwidth, see Appendix A).

For this scenario, we consider all of the scheduling methods defined above. We also introduce a variation of *Spatial Shifting*, in which we do not persistently store data transferred when migrating (S). For *Temporal Shifting* (T) and *Spatio-Temporal Shifting* (TSP), the deadline is either its periodicity or, for ad hoc jobs, a tunable delay tolerance parameter.

## 5. Evaluation

In this section, we provide the experimental setup, data sources, and simulation parameters.

Type	vCPU	Mem (GB)	Bandwidth (Mbps)
c.	1, xl, xxl	2, 4, 8	4, 8, 16
m4.	1, xl, xxl	2, 4, 8	8, 18, 34
r4.	1, xl, xxl	2, 4, 8	16, 32, 65

Table 3: AWS VM instance types and specifications

Region	Location	PUE	WUE	Land Occup. (sqm)
us-east-1	Virginia	1.15	0.12	233101
us-west-1	California	1.17	0.51	116550
eu-central-1	Frankfurt	1.35	0.01	116550
eu-west-2	London	1.11	0.04	116550
eu-north-1	Stockholm	1.10	0.02	116550

Table 4: AWS data by Region for Scenario 2.

### 5.1. Experimental Setup

*Hardware and Software Environment.* The experiments were conducted on the following system:

- *CPU:* Intel(R) Core(TM) i9-10920X CPU @ 3.50GHz
- *RAM:* 260 GB
- *Operating System:* Ubuntu 24.04.3 LTS

*Grid Data and Intensities.* We collected data from various sources. Since we considered multiple regions, we collected publicly available data from different grid operators (see Appendix A). The historical mix data is used to compute the actual environmental impact of the workload execution. Meanwhile, noised mix data is used to simulate the prediction of the grids’ mix that the schedulers optimize their decisions on. The data sources are not standardized, thus we had to harmonize the data to have a common format. We considered a granularity of 1 hour, and finer-grained time series were reshaped considering the mean value for each hour. Table 5.1 depicts the relationship between grids and cloud providers’ regions.

To incorporate uncertainties into the grid mix data, we introduce synthetic noise. Specifically, for each time step and region, the renewable share is perturbed by an error term  $\epsilon_r$  sampled from a normal distribution  $\mathcal{N}(0, \sigma_r)$ , where  $\sigma_r = mae \cdot \frac{1}{\sqrt{2/\pi}}$  and  $mae$  is the target mean absolute error. The error  $\epsilon_r$  is then distributed among the renewable sources (solar, wind, geothermal, hydro, biomass) according to a probability distribution designed to reflect their prediction difficulty: solar gets 45% of error, since it is the hardest source to estimate [30]; wind gets 30% [31]; both hydro [32] and geothermal [33] get 10%; and biomass get 5% of the error, being the most controllable among the renewable sources. Each renewable source  $i$  receives a

noise  $\epsilon_i = \epsilon_r \cdot w_i$ , where  $w_i$  is the weight for source  $i$ . This approach is an attempt to simulate realistic prediction errors and reflects the varying uncertainty associated with each energy source. For non-renewable sources, a uniform noise is applied to each share to maintain the total mix balance.

Finally, in our simulations, to compute the average intensities of the mixes, we consider the intensity coefficients reported in Table 5.1. Carbon intensity values correspond to the median of the lifecycle emissions reported in IPCC Annex III, Table IPCC A.III.2 table (page 1335) [20]. For the oil carbon intensity, which is missing in this source, we consider another coefficient[34]. Water intensity values were obtained from the Water Consumption Factors presented in Tables 1 and 2 (pages 12-13) of the NREL technical report on energy-related water consumption [21]. Land use intensity values were extracted from a comprehensive survey [22]. The survey does not provide a value for oil, but the authors assume it to be comparable to gas, so we did as well. For all the factors, when multiple options were presented for the same energy source, we considered the average of median intensity values. Note that we could not find any source for the oil EWIF; thus, we assume the mean of the other sources’ intensity values. As well as for the unknown share.

*Other Parameters.* For both scenarios we considered the mid-season one-week horizon, from the midnight of the 15th to the midnight of the 22nd, considering the UTC time zone, and varied the week in different seasons, namely: winter (January), spring (April), summer (July), autumn (October). And the step  $\delta_t$  is set to one minute.

To account for the uncertainty in the prediction of the workload, we considered different values of MAE, namely: 0.05, 0.1, 0.15, and 0.2. For statistical significance, each simulation is repeated 6 times with different random seeds, namely: 0, 1, 2, 3, 4, 5.

The factors’ weights are set to: [1.0, 0.0, 0.0], only carbon footprint is optimized, [0.0, 1.0, 0.0], only water footprint is optimized, [0.0, 0.0, 1.0], only land footprint is optimized, [0.333, 0.333, 0.334], all footprints are optimized equally.

Moreover, to account for the energy consumption of the network, we considered a network energy intensity of 0.06 kWh/GB [35]. Finally, we set  $P_d^{IT}$  to the estimate provided by EIA. Assuming the IT power draw to be 100 MW, we assumed an IT power consumption of  $8760 * 100 * 10^3$  kWh over one year.

## 6. Results

In this section, we present the results of our experiments.

### 6.1. Scenario 1: Azure and FaaS

For this first scenario, we present the results of the spatial shifting approach optimizing for all factor weight

	sw	uk	de	
EU	eu-north-1 swedencentral	eu-west-2	eu-central-1	
USA	ercot	miso	pjm	caiso
	southcentralus	centralus	us-east-1 eastus2	us-west-1

Table 5: Data sources for grid mixes

<i>Energy Source</i>	<i>CI</i> <i>gCO2e/kWh</i>	<i>EWIF</i> <i>l/kWh</i>	<i>ELIF</i> <i>ha/TWh</i>
Nuclear	12	1.957	7.1
Geothermal	38	5.827	45
Biomass	485	1.145	29065
Coal	820	1.8	1000
Wind	11.5	0	6065
Solar	38.67	1.385	1650
Hydro	24	17	650
Gas	490	1.099	1155
Oil	720	n/a (3.776)	1155
Unknown	n/a (293.24)	n/a (3.776)	n/a (4532)

Table 6: Impact coefficients for various electricity generation technologies. *Sources*: Carbon: IPCC [20], Our World in Data [34] (oil). Water: NREL [21]. Land use [22].

combinations.

*Spatial Shifting.* Figure 1 shows the footprint improvement with respect to the local baseline of spatial shifting. This experiment considered the winter week and an error of 10% on the renewable share prediction. We compare all factor weights' combinations defined above.

The results demonstrate that regional shifting of FaaS workloads across Azure regions leads to noticeable improvements in carbon efficiency. The plots show that when optimizing for a particular metric (carbon, water, or land use footprint), we can achieve a 45 – 85% improvement in that metric. When considering the metric for which the optimization was performed, we see that the carbon footprint benefits the most, with up to an 85% reduction in emissions compared to the local baseline. This significant reduction reflects the negligible migration cost of FaaS workloads. A reduction of about 85% in carbon footprint leads to an increase of about 40% in water footprint. The land use footprint also increases, but to a lesser extent, having observed about a 25% increase.

Similarly, optimizing for water footprint (about 50% reduction) leads to a significant increase in carbon footprint (about 125% increase), but the land use footprint decreases proportionally to the water footprint reduction (about 50% reduction). On the other hand optimizing for land use footprint (about 45% reduction) leads to a moderate increase in carbon footprint (about 15% increase) and a small reduction in water footprint (less than 10% reduction).

Figure 2 shows the request distribution across the regions. To help us understand this distribution, let us consider Figure 3, which simultaneously reports intensity values over the winter week and the efficiency metrics for each factor for each region.

When optimizing for carbon, all the requests are scheduled to "centralus" which is not the most energy-efficient region (PUE 1.172), and it has the grid with the lowest carbon intensity. When optimizing for water, a small percentage of requests go to "eastus2" and most of the requests are scheduled to "centralus", which is not the most water-efficient region (WUE 0.19) nor is it the one with the smallest grid water intensity. However, it is the region with the lowest impact on water when considering both data center efficiency and grid intensity. Finally, when optimizing for land use, nearly all the requests are scheduled to "eastus2", which, even if it is not the region with the least land occupation, its grid has a lower land use intensity.

*Sensitivity Analysis.* To understand how seasonality affects the effectiveness of the scheduling methods, we perform a sensitivity analysis considering weeks in the four seasons: winter, spring, summer, and autumn. For this analysis, we use a fixed error for the grid's renewable share prediction ( $mae = 0.1$ ). On the other hand, to understand how the prediction error affects the effectiveness of the scheduling methods, we perform a sensitivity analysis considering different values of prediction error ( $mae = \{0.05, 0.1, 0.15, 0.2\}$ ). We use a fixed week in winter for this analysis.

From Tables 9 and 9, it is possible to notice that the prediction error leads to very small differences, almost flat. Indeed, the results indicate that the improvement in reduction in all three metrics remains robust even for higher error levels.

On the other hand, it seems that the effectiveness of spatial shifting varies with seasonal changes in grid intensities, but the overall trend of improvement remains consistent. Land use factors, in particular, demonstrate varying impacts across different seasons (37%-57%).

## 6.2. Scenario 2: AWS and Big Data

For this second scenario, not only do we investigate the spatial shifting method, but also temporal shifting and spatio-temporal shifting. We consider the same week in winter as in Scenario 1. We consider a prediction error

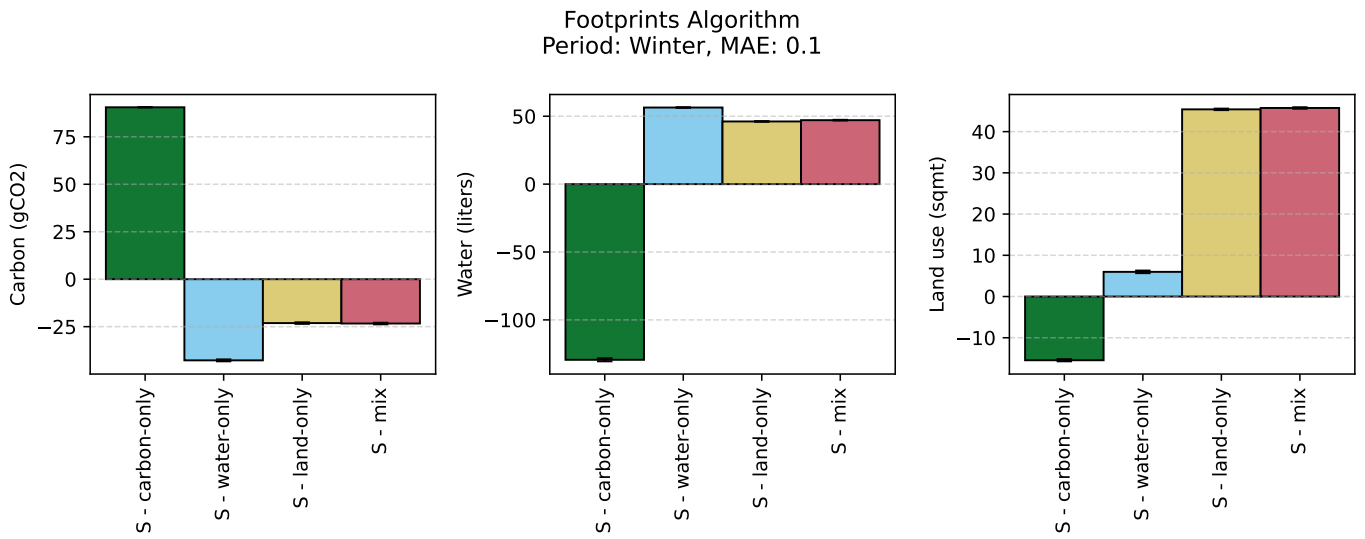


Figure 1: Spatial shifting for Scenario 1; showing a 45 – 85% improvement over local baseline during a winter week, with an MAE of 10%.

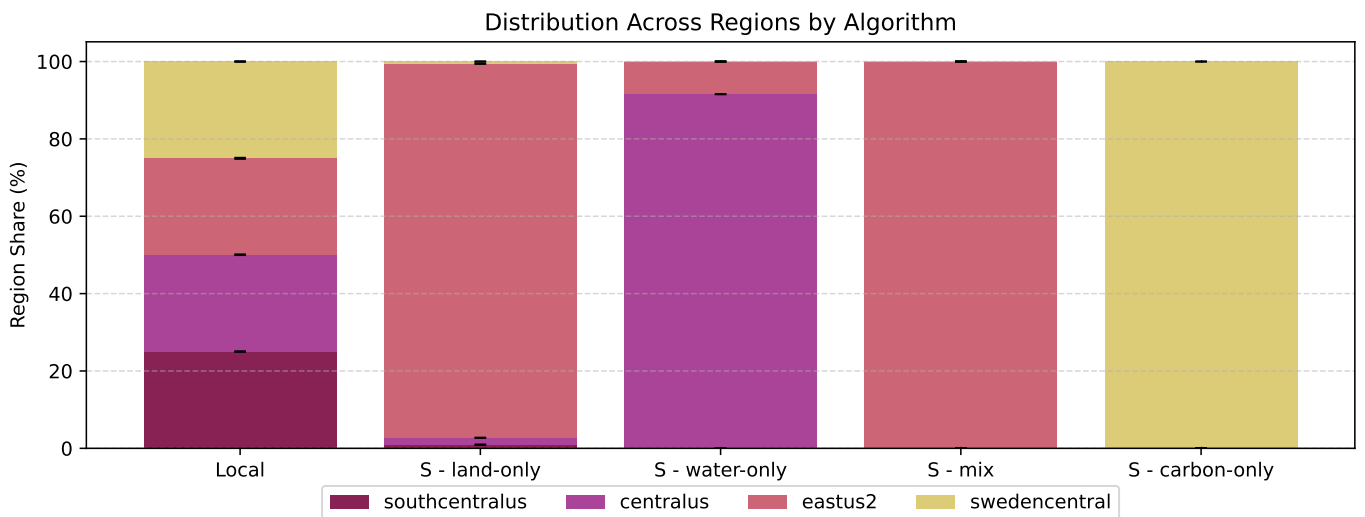


Figure 2: Request distribution across different regions for different criteria for Scenario 1 during a Winter week, with an MAE of 10%.

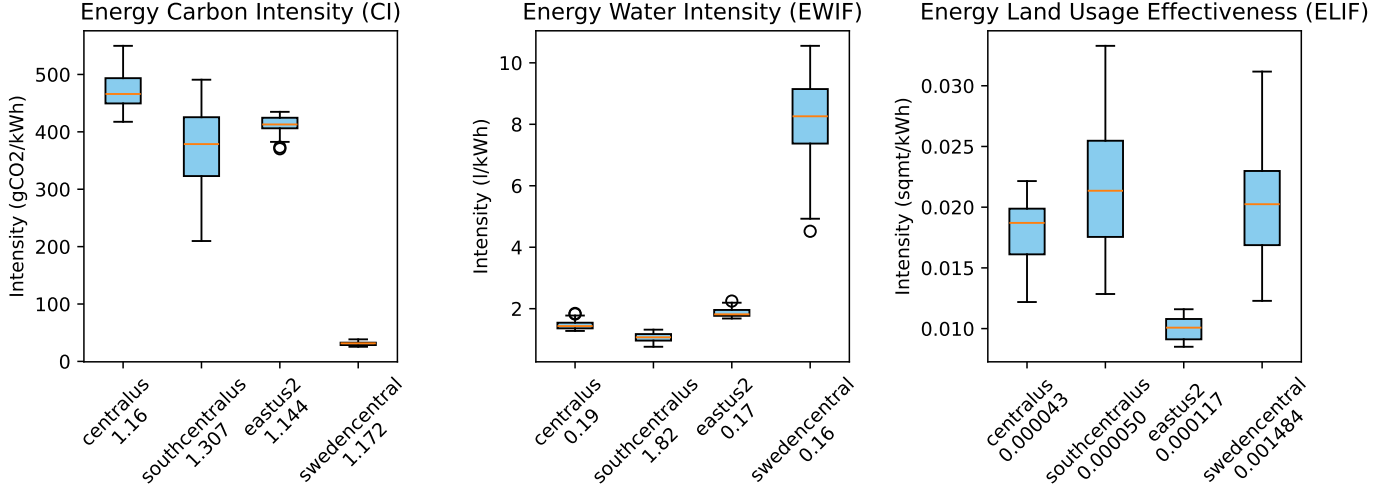


Figure 3: Grid intensities for each factor, and each region for Scenario 1 over a winter week, with an MAE of 10%.

(mae) of 0.1. We consider the same factor weights' combinations as in Scenario 1. For temporal shifting, we consider different values of delay tolerance ( $dt$ ) = {4, 12, 24, 48} hours.

*Baseline Footprints.* The baseline algorithm (Local) has about 17.500 kilograms of carbon footprint, 200.000 liters of water footprint, and just above 2000 square meters of land use footprint. In these graphs, we show the improvement in percentage of the other algorithms with respect to the baseline. Figure 4 shows the results of our experiments.

*Temporal Shifting.* Firstly, we can see that the temporal shifting approach achieves relatively modest improvements compared to spatial shifting, with reductions ranging from 6% to 12% even at the highest delay tolerance of 48 hours.

*Spatial Shifting.* The spatial shifting approach (SP) achieves a significant improvement in each metric when optimizing for it. In this case, the improvements range from 20 – 45% footprint reductions over the baseline. Figure 5 shows the request distribution across the regions. To help us understand this distribution, let us consider Figure 6, which simultaneously reports intensity values over the winter week and the efficiency metrics for each factor for each region.

When optimizing for carbon, about 50% of requests are scheduled to "eu-north-1", which is the most energy-efficient region (PUE 1.1) and also the region with the grid with the lowest carbon intensity. When optimizing for water, about 40% of requests are scheduled to "us-west-2", which is not the most water efficient region (WUE 0.04), but it has the grid with the lowest impact on water. Finally, when optimizing for land use, about 45% of requests are scheduled to "us-east-1", which, even if it is the region with the most land occupation, it is the one where the grid has the lowest impact on land use.

	Carbon (%)		Water (%)		Land Use (%)	
	S	SP	S	SP	S	SP
carbon-only	12.67	6.96	3.45	1.80	7.68	4.13
water-only	3.50	1.85	5.47	2.94	3.07	1.58
land-use-only	3.51	1.80	4.55	2.60	6.62	3.65
mix	1.69	0.85	1.67	0.89	1.89	1.01

Table 7: Spatial shifting (persistent storage vs non-persistent storage) average percentage of migration footprints for Scenario 2 during Winter week, with an MAE of 10%.

*Migration Overheads of Spatial Shifting.* For this scenario, we also consider an alternative approach to spatial shifting (S). In this approach, the data associated with each request must be transferred each time a migration occurs, even if the data was transferred to that region previously. Results show that this approach still achieves significant improvements over the baseline, but SP achieves about 5 – 6% better results in the optimized metric.

Table 6.2 provides a summary of the migration overhead for the three factors; it shows the percentage of footprints caused by migration. The migration overhead varies based on the scheduling algorithm and the weights used, ranging from 0.85% to 12.67% for carbon, 0.89% to 5.47% for water, and 1.01% to 7.68% for land use. The overhead of SP is about half compared to S.

*Spatio-Temporal Shifting.* Finally, the best outcome is achieved by the spatio-temporal shifting approach (STP) with a delay tolerance of 4 hours, which results in 55% improvement in carbon footprint when optimizing for carbon, about 40% improvement in water footprint when optimizing for water, and about 48% improvement in land use footprint when optimizing for land use. However, these im-

Footprints Algorithm  
 Period: Winter, MAE: 0.1

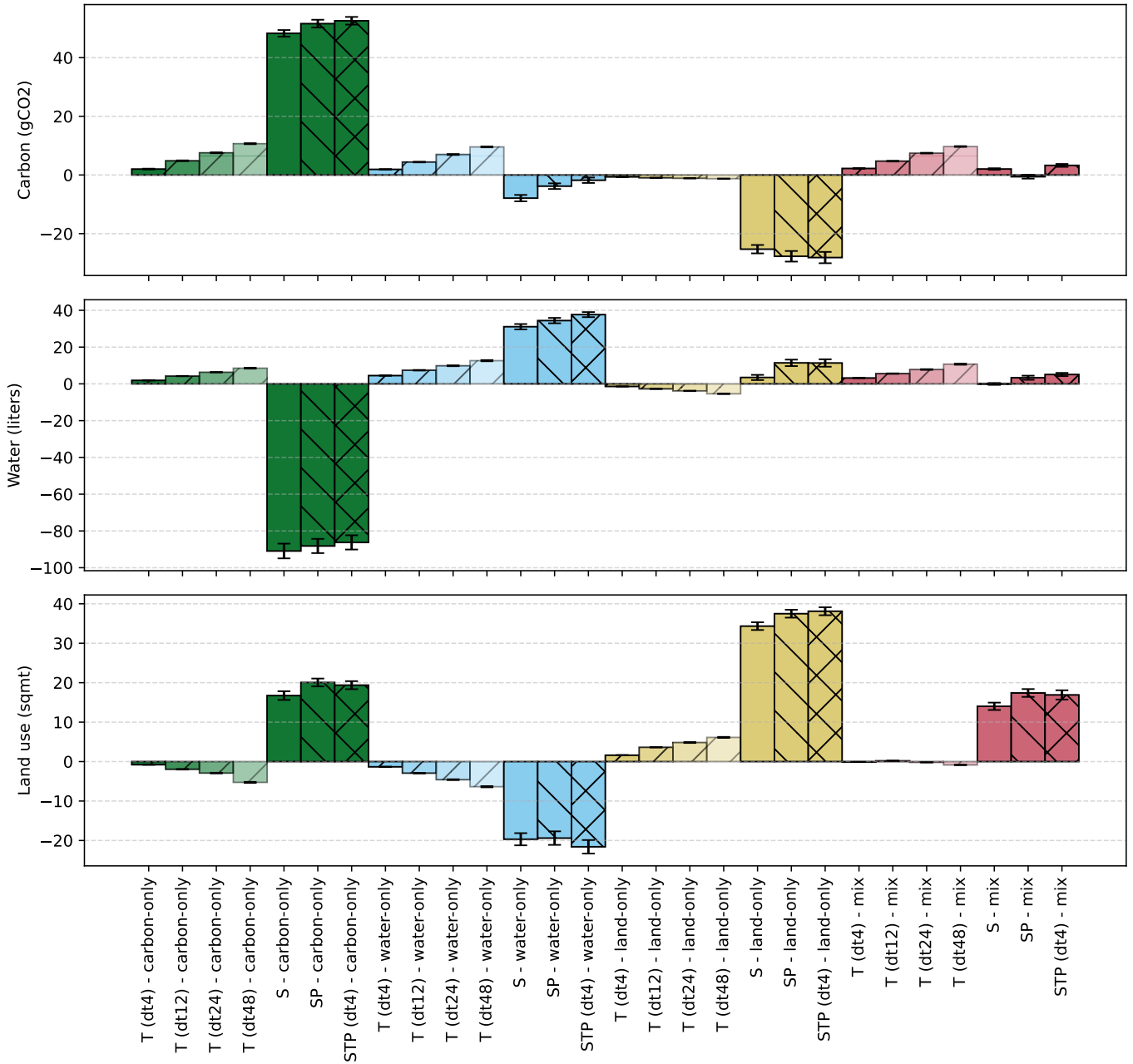


Figure 4: Temporal, spatial, and spatio-temporal shifting for Scenario 2 improvement over local baseline results, with an MAE of 10%. Temporal shifting shows 6 – 12% improvement; spatial shifting comes in at 20 – 45%; while combining both gives the best result of 40 – 55% improvement over the baseline.

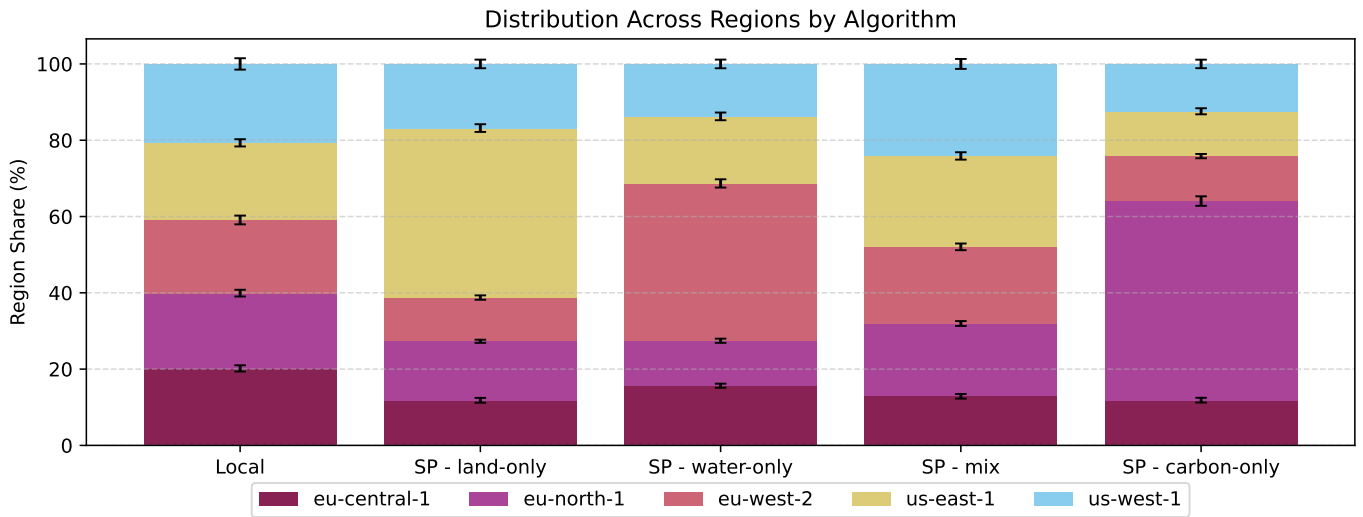


Figure 5: Request distribution across different regions for different criteria for Scenario 2 during a Winter week, with an MAE of 10%.

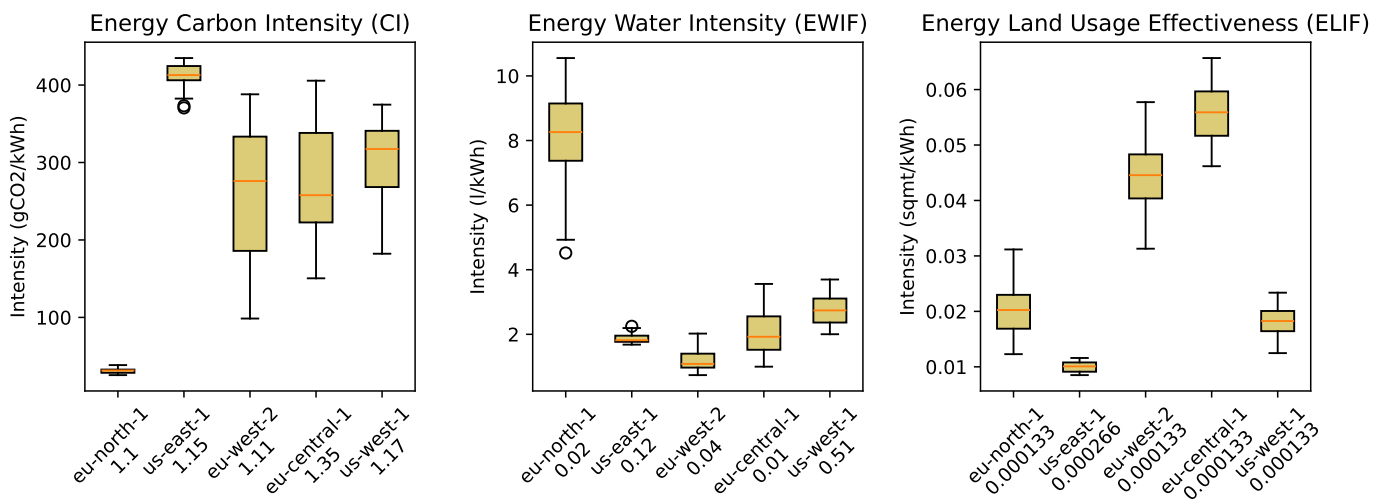


Figure 6: Grid intensities for each factor, and each region for Scenario 2 over a winter week, with an MAE of 10%.

provements with respect to only spatial shifting are small.

*Sensitivity Analysis.* Following the same approach used for Scenario 1, we conduct sensitivity analysis for this scenario as well. Tables 9 and 9 respectively show the footprint improvements over the local baseline for different seasons and for different prediction errors for the grid renewable share (mae). The results fluctuate slightly with the prediction error (2-3%), but the improvements remain significant even with a high prediction error of 0.2. Also, the season does not affect the results significantly, with variations of 4% at most, considering the optimized factor.

## 7. Discussion

In this section, we discuss the results obtained.

### 7.1. Scenario 1: Azure and FaaS

The results demonstrate that regional shifting of FaaS workloads across Azure regions leads to noticeable improvements in carbon efficiency.

Overall, these results highlight the potential of spatial shifting to significantly enhance the sustainability of FaaS workloads by leveraging regional variations in grid intensities and regional efficiency differences. This suggests that lightweight workloads such as FaaS functions could serve as a first mover for sustainability-aware orchestration, as they can be shifted freely without incurring significant migration penalties. Our results show that accounting for provider-declared PUE/WUE improves allocation decisions, especially when grid mixes are similar. This highlights that relying solely on grid intensity overlooks potential sustainability gains and the importance of region-specific data center disclosures for enabling sustainability-aware workload management.

### 7.2. Scenario 2: AWS and Big Data

The results highlight the potential of spatial shifting to significantly enhance the sustainability of cloud workloads by leveraging, for the most part, regional variations in grid intensities. However, the migration overhead is relevant, especially when data is not persistently stored after migration. Nevertheless, the benefits of spatial shifting in reducing the overall footprint outweigh the footprints associated with migration, obtaining a substantial footprint improvement. Combined spatial and temporal shifting can lead to even more significant improvements, although the additional benefits are relatively modest compared to spatial shifting alone. This suggests that while temporal shifting can contribute to sustainability goals, its impact is limited by the inherent variability of renewable energy availability within a single region. Though it is worth noting that even if temporal shifting has less savings, it does not require to move data between regions, which sometimes will not be possible due to security/privacy concerns.

These findings reveal a trade-off: although spatial shifting yields the greatest reductions, it may be limited in practice by sovereignty, privacy, and cost constraints. Therefore, temporal shifting is an important alternative, despite its standalone benefits being smaller; it can be applied even when workloads cannot be transferred to another region. This suggests prioritising spatial shifting for portable workloads and using temporal shifting as a fallback for constrained ones.

### 7.3. Comparison of the Two Scenarios

From the results, we can see that with diverse providers and workloads, the results are different, but the improvements are relevant in both. In particular, we can see that for the Azure-based scenario we obtain the greatest improvements, since there is no footprint overhead when migrating, while for the AWS-based scenario, there can be relevant overhead, e.g., 12% carbon footprint related to data transfer. However, this overhead is such that the improvements are still significant. Moreover, it allows us to obtain a more balanced distribution of requests among the regions.

### 7.4. Trade-Off Analysis

As expected, in both scenarios, optimizing for one metric can lead to trade-offs in the other metrics. For instance, optimizing for carbon footprint leads to a significant increase in water footprint, as already observed in previous studies [18].

This is particularly evident when optimizing for carbon, which results in a significant increase in water footprint. Optimizing for water results in an increase in both carbon and land use footprints, but to a lesser extent compared to the increase in water footprint when optimizing only for carbon. Optimizing for the mix of the three factors results in a balanced reduction of all three footprints, but the improvements are lower compared to optimizing for only one factor.

To help us understand these trade-offs, we consider the energy intensity factors for each energy source. Figure 7 shows the energy intensity factors normalized between 0 and 1 (by dividing by the sum of each factor across all sources). It seems that carbon and water are negatively correlated (e.g., hydro, coal), but not all low-carbon-intensity sources have high water intensity (e.g., wind and nuclear). On the other hand, land use seems to not be correlated with the other factors, although there are sources with high land use and low water intensity (e.g. biomass), and sources with low land use and high carbon and water intensity (e.g. oil).

### 7.5. Threats to Validity

This study presents some threats to validity that should be considered when interpreting the results.

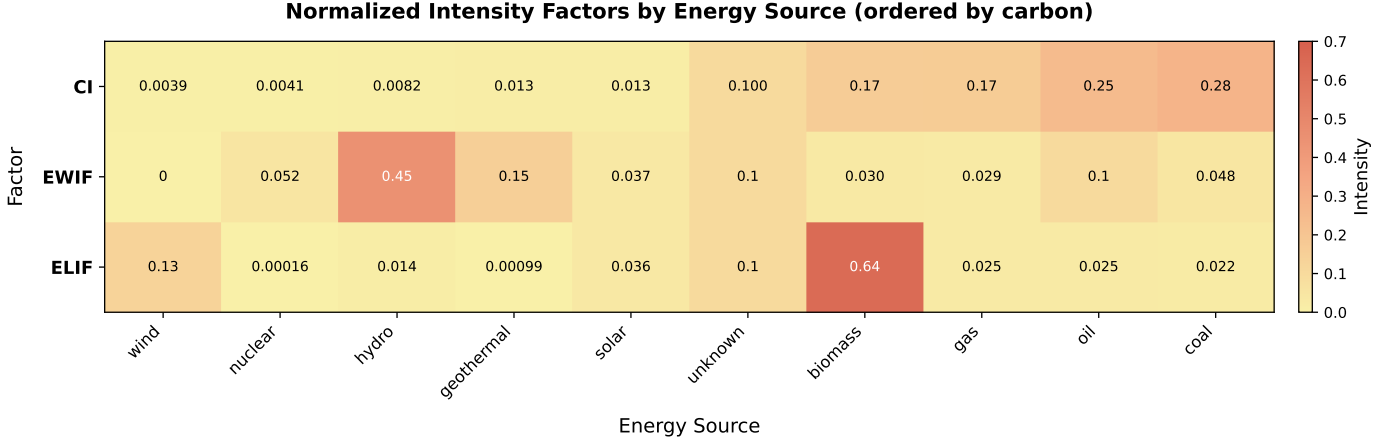


Figure 7: Normalized energy intensity factors for each energy source, showing a negative correlation between carbon and water, and seemingly no correlation between land and the other factors.

*Resource availability.* We assume that there are always resources available, which might not be true in reality. However, considering the promise of elastic scalability of public cloud providers and general availability of surplus “spot” resources, this appears to be a sensible assumption.

*Generality.* The scenarios considered may not fully represent the diversity of real-world cloud environments, as we focused on specific providers (Azure and AWS) and workload types (FaaS and big data). Moreover, the workload traces used for the AWS-based scenario may not be representative of production cloud workloads since arrival patterns are synthetically randomized. However, we selected two diverse cases: lightweight, latency-sensitive workloads (FaaS) and scalable data-intensive batch processing (big data). The fact that we observe similar trade-offs across such different cases increases the confidence that the results generalize, even though more workload classes should be studied in future work.

*Input Data Quality.* The accuracy of our results is contingent upon the quality of the input data, including grid mix predictions. In our case, these predictions were mimicked using historical data and applying an arbitrary noise distribution. Moreover, to estimate the LUE parameter, we use estimations for the region’s IT power consumption and the land occupation, since precise data is not available. These approximations could affect the validity of our findings, yet this data is unfortunately not freely and openly available. Finally, it is assumed that the application runtimes are available to the schedulers. While it is not necessarily realistic to know these runtimes exactly prior to executions, low-error estimates could be available from previous runs or profiling [36, 37, 38, 39].

*Spatial Shifting Constraints.* Our models assume that workloads can be shifted across regions and time without considering potential constraints such as latency requirements, data sovereignty issues, or privacy concerns. While

these issues are significant, they primarily affect spatial shifting. Temporal shifting, in contrast, only delays the execution, and all data can remain in the same location.

*Economic Costs.* Our simulations do not account for potential economic costs associated with shifting workloads geographically. In practice, migrating data between data center locations can introduce significant costs, which would need to be considered. Meanwhile, we assume that the cost of storing data for longer for delaying executions has a negligible monetary cost.

## 8. Related Work

Research into cloud orchestration has generated a substantial body of work aimed at improving resource management and operational efficiency [40]. Within this space, two areas have attracted considerable attention: optimizing energy consumption and incorporating carbon awareness into system design [10, 13, 4, 12, 5, 15, 11, 6, 9, 16].

Recently, the impact on water resources of computation has also raised concerns, but few studies have focused on this issue [17, 18]. Different from previous works, we also included land use in an approach that simultaneously assesses and optimizes the overall impact in terms of carbon, water, and land use footprint.

### 8.1. Carbon-Aware Computing

In cloud computing, carbon-aware optimization focuses on aligning workload execution with variations in the carbon intensity of the electricity supply over time and/or across different geographical areas.

*Temporal Shifting.* In [10], we analyse the temporal shifting benefits considering different regions, demonstrating the carbon savings potential of delay-tolerant workloads in Germany, Great Britain, France, and California.

Hanafy et al. [9] propose CarbonScaler, where cloud batch jobs dynamically adjust server allocations based on

grid carbon intensity, and demonstrate the performance of this approach in a Kubernetes prototype.

Piontek et al. [11] introduce a carbon-aware Kubernetes scheduler that leverages a prediction algorithm to defer non-critical workloads in time, thereby reducing overall carbon emissions.

*Spatial Shifting.* Gao et al. [4] present a scheduler that manages traffic distribution across data centers, balancing a three-way trade-off among access latency, electricity cost, and carbon footprint.

Building on the idea of geo-distributed scheduling, Maji et al. [5] propose a load balancing solution for VMware’s Avi Global Server Load Balancer, employing a linear scoring function to select the most suitable data center based on marginal carbon intensity and client-to-data-center distance.

Similarly, Chadha et al. [6] introduce GreenCourier, a Kubernetes scheduler aimed at curbing the carbon emissions of serverless functions deployed across geographically distributed regions.

Lindberg et al. [7] propose a metric, named locational marginal carbon emission, to guide spatial shifting.

Zheng et al. [8] evaluate the idea of migrating workloads between data centers to reduce curtailment. It has been shown that migrating workloads from fossil-fuel-powered grids to renewable-energy-powered grids during curtailment hours simultaneously reduces emissions and absorbs excess renewable generation.

*Spatio-Temporal Shifting.* Zhou et al. [12] apply Lyapunov optimization to jointly perform load balancing across geo-distributed data centers, capacity right-sizing through powering down idle servers, and server speed scaling via CPU frequency adjustment, with the goal of balancing a three-way trade-off among electricity cost, SLA requirements, and emission reduction targets.

Souza et al. [13] propose a provisioner that simultaneously minimizes the number of active servers and their associated carbon emissions.

Sukprasert et al. [14] examine the benefits and limitations of carbon-aware spatiotemporal shifting for cloud workloads, offering insight into its practical applicability.

Cordingly et al. [15] introduce a prototype for computing resource aggregation that reduces the carbon footprint of serverless applications through carbon-aware load distribution.

Lin et al. [16] propose a coordinated scheduling framework that aligns data center capacity planning with grid dynamics in both spatial and temporal dimensions to avoid increasing carbon emissions, energy costs, and reducing grid reliability.

## 8.2. Beyond Carbon-Aware Computing

Recent research has begun broadening the scope of environmental impact assessment for cloud and AI workloads beyond carbon emissions alone.

Li et al. [17] shed light on the often-overlooked water footprint of AI models, revealing the substantial freshwater consumption associated with both cooling systems and electricity generation, and estimating that training large AI models can result in hundreds of thousands of liters of direct water use.

Jiang et al. [18] propose WaterWise, a job scheduling framework that co-optimizes carbon and water sustainability across geographically distributed data centers. Their approach relies on a Mixed Integer Linear Programming (MILP)-based scheduler that dynamically routes workloads to regions with favorable carbon and water conditions, while respecting delay tolerance constraints. This line of work resonates with our own, which similarly advocates for multi-dimensional sustainability metrics in cloud workload allocation and underscores the need for comprehensive, sustainability-aware orchestration strategies.

Within prior literature, [18] is the closest to our work. While WaterWise represents an important step toward integrating water sustainability, its methodology suffers from two major limitations: it simplifies regional operational characteristics by assuming constant data center efficiency (PUE set to 1.2 for all regions), and it relies on a linear regression based on the wet-bulb temperature for estimating WUE values. As shown in our previous work[41], this method can lead to estimations that differ substantially from the values declared by the providers, probably because it derives from a study conducted on a specific cooling technology [42]. Instead, we focus more on regional differences beyond grid intensities using both region-specific PUE and WUE values declared by providers. Furthermore, to the best of our knowledge, land use has not previously been considered alongside carbon and water footprints in cloud workload allocation.

## 8.3. Comparison With Own Previous Work

We presented the idea of holistic sustainable cloud workload allocation at the 1st International Workshop on Low Carbon Computing [41]. Unlike our workshop paper, this paper focuses specifically on carbon, water and land use as highly relevant yet increasingly assessable impact factors. Furthermore, we also include temporal shifting, and we no longer assume workloads can be migrated live and without costs, but instead focus on spatial shifting of workloads prior to their execution in our simulations. Moreover, to ensure the relevance of our simulations, we use real-world workload traces instead of synthetic data to simulate jobs in this paper.

We have also previously worked on carbon-aware temporal load shifting [10], as well as admission control policies [43] and client selection strategies [44] to leverage renewable excess energy for machine learning workloads. Similarly, we have published results on carbon-aware scheduling and scaling of scientific workflows [45]. However, these works aim exclusively at reducing carbon emissions and do not consider water or land use efficiencies.

## 9. Conclusion

In this paper, we have demonstrated that spatial and temporal shifting can significantly reduce the environmental footprint of cloud workloads in terms of carbon emissions, water consumption, and land use. Spatial shifting, in particular, has yielded substantial improvements across all three environmental factors considered, with reductions ranging from 20% to 85% depending on the scenario and optimization criteria. Temporal shifting also contributes to footprint reduction, albeit to a lesser extent, with improvements of up to 12%. However, since temporal shifting does not require workloads to be migrated between regions, it may be more relevant in practice, when migration is restricted for data privacy or cost reasons. The combination of both methods yields the highest reductions, although the incremental benefit over spatial shifting alone is relatively small.

Our sensitivity analyses indicate that both shifting methods are robust to prediction errors in grid mix data and maintain their effectiveness across different seasons. Finally, we have demonstrated that it is possible to reduce the environmental footprint and mitigate trade-off implications by optimizing multiple impact factors simultaneously using a mixed strategy. Overall, our findings highlight the potential of a more sustainable workload scheduling as a practical approach considering diverse cloud providers and workloads.

In the future, we would like to study the impact of cross-region availability, load balancing, and low-latency requirements. In addition, beyond shifting, we are keen to further explore the role of resource configurations and dynamic scaling when carbon, water, and land use are jointly optimized for cloud workloads. Finally, it would be interesting to incorporate the concept of “water stress” to reflect the varying impact that water consumption can have on areas with different hydrogeological characteristics to provide a more equitable representation of the environmental trade-off across regions. Similarly, a concept of “land-use stress” could be introduced to better reflect the environmental impact of data center developments in different geographical areas.

## Acknowledgments

This work was supported by the Engineering and Physical Sciences Research Council under grant number UKRI154 (“Casper: Carbon-Aware Scalable Processing in Elastic Clusters”).

## Rights Retention

For the purpose of open access, we have applied a Creative Commons Attribution (CC BY) licence to any Author Accepted Manuscript version arising from this submission.

## References

- [1] C. Freitag, M. Berners-Lee, K. Widdicks, B. Knowles, G. S. Blair, A. Friday, The real climate and transformative impact of ict: A critique of estimates, trends, and regulations, *Patterns* 2 (9) (2021).
- [2] L. Belkhir, A. Elmeligi, Assessing ict global emissions footprint: Trends to 2040 & recommendations, *Journal of cleaner production* 177 (2018).
- [3] Energy and ai, Tech. rep., IEA, accessed: 2026-02-20 (2025).  
URL <https://www.iea.org/reports/energy-and-ai>
- [4] P. X. Gao, A. R. Curtis, B. Wong, S. Keshav, It’s not easy being green, in: *Proceedings of the ACM SIGCOMM 2012 Conference on Applications, Technologies, Architectures, and Protocols for Computer Communication, SIGCOMM ’12*, ACM, 2012.
- [5] D. Maji, B. Pfaff, V. P R, R. Sreenivasan, V. Firoiu, S. Iyer, C. Josephson, Z. Pan, R. K. Sitaraman, Bringing carbon awareness to multi-cloud application delivery, in: *Proceedings of the 2nd Workshop on Sustainable Computer Systems, HotCarbon ’23*, ACM, 2023.
- [6] M. Chadha, T. Subramanian, E. Arima, M. Gerndt, M. Schulz, O. Abboud, Greencourier: Carbon-aware scheduling for serverless functions, in: *Proceedings of the 9th International Workshop on Serverless Computing, WoSC ’23*, ACM, 2023.
- [7] J. Lindberg, Y. Abdennadher, J. Chen, B. C. Lesieutre, L. Roald, A guide to reducing carbon emissions through data center geographical load shifting, in: *Proceedings of the Twelfth ACM International Conference on Future Energy Systems, e-Energy ’21*, ACM, 2021.
- [8] J. Zheng, A. A. Chien, S. Suh, Mitigating curtailment and carbon emissions through load migration between data centers, *Joule* 4 (10) (2020).
- [9] W. A. Hanafy, Q. Liang, N. Bashir, D. Irwin, P. Shenoy, Carbonscaler: Leveraging cloud workload elasticity for optimizing carbon-efficiency, *Proc. ACM Meas. Anal. Comput. Syst.* 7 (3) (Dec. 2023).
- [10] P. Wiesner, I. Behnke, D. Scheinert, K. Gontarska, L. Thamsen, Let’s wait awhile: how temporal workload shifting can reduce carbon emissions in the cloud, in: *Proceedings of the 22nd International Middleware Conference, Middleware ’21*, ACM, 2021.
- [11] T. Piontek, K. Haghshenas, M. Aiello, Carbon emission-aware job scheduling for kubernetes deployments, *Journal of supercomputing* 80 (2023).

algorithm	period	carbon		water		land use	
		improvement mean	std	improvement mean	std	improvement mean	std
S - carbon-only	autumn	91.28	0.03	-118.26	0.75	-8.10	0.46
	spring	86.56	0.04	-139.90	1.17	18.29	0.32
	summer	91.87	0.02	-123.28	1.15	-13.85	0.29
	winter	90.55	0.03	-129.41	1.12	-15.46	0.26
S - water-only	autumn	-48.74	0.55	55.33	0.22	6.57	0.35
	spring	-29.97	0.39	59.40	0.19	-11.63	0.41
	summer	-24.66	0.39	50.82	0.21	32.46	0.13
	winter	-42.75	0.52	56.42	0.23	5.99	0.32
S - land-only	autumn	-25.17	0.50	40.90	0.30	57.00	0.17
	spring	-15.63	0.35	34.32	0.37	42.24	0.22
	summer	-13.88	0.41	39.31	0.36	37.54	0.12
	winter	-23.12	0.42	46.16	0.27	45.40	0.19
S - mix	autumn	-25.86	0.49	42.35	0.27	57.16	0.17
	spring	-23.35	0.35	49.22	0.24	42.73	0.22
	summer	-17.64	0.40	49.55	0.23	38.33	0.12
	winter	-23.34	0.43	47.10	0.28	45.74	0.18

Table 8: Scenario 1 - Season sensitivity analysis

algorithm	mae	carbon		water		land use	
		improvement mean	std	improvement mean	std	improvement mean	std
S - carbon-only	0.05	90.55	0.03	-129.41	1.12	-15.46	0.26
	0.1	90.55	0.03	-129.41	1.12	-15.46	0.26
	0.15	90.55	0.03	-129.41	1.12	-15.46	0.26
	0.2	90.55	0.03	-129.41	1.12	-15.46	0.26
S - water-only	0.05	-43.64	0.52	56.60	0.23	4.95	0.32
	0.1	-42.75	0.52	56.42	0.23	5.99	0.32
	0.15	-42.81	0.51	56.25	0.23	6.79	0.32
	0.2	-41.36	0.51	55.84	0.23	8.59	0.30
S - land-only	0.05	-23.40	0.43	47.12	0.28	45.71	0.18
	0.1	-23.12	0.42	46.16	0.27	45.40	0.19
	0.15	-22.33	0.42	44.14	0.29	44.85	0.18
	0.2	-22.03	0.42	42.84	0.30	44.15	0.19
S - mix	0.05	-23.34	0.43	47.10	0.28	45.74	0.18
	0.1	-23.34	0.43	47.10	0.28	45.74	0.18
	0.15	-23.34	0.43	47.10	0.28	45.74	0.18
	0.2	-23.32	0.43	47.08	0.28	45.57	0.18

Table 9: Scenario 1 - Mix renewable share prediction error sensitivity analysis

algorithm	period	carbon		water		land use	
		improvement mean	std	improvement mean	std	improvement mean	std
SP carbon-only	autumn	52.00	1.33	-65.81	2.96	21.26	0.86
	spring	45.96	1.11	-68.89	2.95	30.19	0.89
	summer	51.05	1.34	-70.26	3.13	29.75	0.90
	winter	51.60	1.32	-88.18	3.86	20.05	1.00
SP water-only	autumn	-3.02	0.88	32.83	1.16	-18.67	1.57
	spring	-0.53	0.81	32.77	1.32	-20.88	1.64
	summer	-27.04	2.13	29.59	1.20	9.16	1.38
	winter	-3.81	0.96	34.42	1.46	-19.40	1.72
SP land-only	autumn	-25.84	2.05	11.83	1.63	41.04	1.02
	spring	-21.40	1.81	-3.26	1.57	38.43	0.98
	summer	-23.65	1.46	2.72	1.45	39.74	1.00
	winter	-27.72	1.81	11.42	1.76	37.49	1.00
SP mix	autumn	1.99	0.90	7.43	1.13	24.13	0.78
	spring	2.78	1.24	15.98	1.67	16.26	1.20
	summer	6.49	0.92	-0.22	1.33	20.48	1.08
	winter	-0.59	0.64	3.33	1.13	17.39	0.99
T (dt4) carbon-only	autumn	5.09	0.26	3.51	0.10	0.59	0.09
	spring	4.28	0.28	2.63	0.16	1.37	0.11
	summer	4.60	0.23	2.00	0.12	1.46	0.17
	winter	2.02	0.14	1.90	0.08	-0.79	0.03
T (dt4) water-only	autumn	4.93	0.24	6.81	0.09	0.32	0.11
	spring	4.62	0.27	6.24	0.16	0.51	0.10
	summer	4.35	0.24	7.26	0.16	0.99	0.13
	winter	1.91	0.11	4.49	0.11	-1.33	0.05
T (dt4) land-only	autumn	1.97	0.23	-0.15	0.13	3.71	0.12
	spring	2.67	0.24	0.48	0.17	3.75	0.14
	summer	2.11	0.20	-0.21	0.09	4.80	0.20
	winter	-0.65	0.04	-1.41	0.05	1.62	0.05
T (dt4) mix	autumn	5.54	0.25	5.49	0.09	1.71	0.13
	spring	5.67	0.29	4.87	0.18	2.74	0.12
	summer	5.24	0.26	5.77	0.15	3.12	0.17
	winter	2.22	0.13	3.19	0.11	-0.10	0.03
STP (dt4) carbon-only	autumn	54.46	1.30	-63.54	3.00	21.24	0.87
	spring	48.67	1.13	-72.15	3.29	31.87	0.91
	summer	53.37	1.34	-71.52	3.22	30.97	0.93
	winter	52.59	1.31	-86.23	3.87	19.37	1.02
STP (dt4) water-only	autumn	1.66	0.83	37.05	1.13	-19.98	1.42
	spring	3.93	0.73	36.43	1.31	-23.77	1.63
	summer	-22.21	1.75	33.30	1.18	6.84	1.07
	winter	-1.79	0.93	37.66	1.38	-21.60	1.72
STP (dt4) land-only	autumn	-23.46	2.02	10.23	1.51	42.53	0.99
	spring	-22.95	2.00	0.64	1.34	40.20	0.96
	summer	-22.05	1.57	2.83	1.15	41.86	1.00
	winter	-28.16	1.93	11.35	2.01	38.11	1.01
STP (dt4) mix	autumn	9.21	1.09	10.30	1.35	24.10	0.82
	spring	12.29	0.55	18.50	1.66	17.32	1.09
	summer	12.86	0.78	3.76	1.42	20.38	0.87
	winter	3.27	0.49	5.09	0.88	16.91	1.17

Table 10: Scenario 2 - Season sensitivity analysis

algorithm	mae	carbon		water		land use	
		improvement mean	std	improvement mean	std	improvement mean	std
SP carbon-only	0.05	51.72	1.32	-88.67	3.86	20.31	0.97
	0.1	51.60	1.32	-88.18	3.86	20.05	1.00
	0.15	51.27	1.34	-86.49	3.91	19.29	0.99
	0.2	49.97	1.25	-81.37	3.67	16.97	0.95
SP water-only	0.05	-3.61	0.95	34.71	1.46	-20.22	1.65
	0.1	-3.81	0.96	34.42	1.46	-19.40	1.72
	0.15	-4.27	1.00	34.16	1.44	-19.20	1.71
	0.2	-4.04	1.04	34.17	1.44	-18.63	1.71
SP land-only	0.05	-28.87	1.87	12.51	1.87	37.73	1.01
	0.1	-27.72	1.81	11.42	1.76	37.49	1.00
	0.15	-27.32	1.71	10.60	1.63	37.32	1.01
	0.2	-25.64	1.57	8.49	1.71	36.78	0.95
SP mix	0.05	0.17	0.56	1.58	1.03	17.69	1.20
	0.1	-0.59	0.64	3.33	1.13	17.39	0.99
	0.15	0.48	0.81	2.75	1.09	16.43	1.40
	0.2	-6.59	1.11	8.37	1.43	19.93	1.29
T (dt4) carbon-only	0.05	2.67	0.15	1.55	0.07	-0.89	0.04
	0.1	2.02	0.14	1.90	0.08	-0.79	0.03
	0.15	1.92	0.13	1.39	0.09	-0.62	0.03
	0.2	1.72	0.11	1.04	0.06	-0.47	0.04
T (dt4) water-only	0.05	2.15	0.12	4.85	0.11	-1.60	0.06
	0.1	1.91	0.11	4.49	0.11	-1.33	0.05
	0.15	1.76	0.11	4.34	0.11	-1.29	0.06
	0.2	1.84	0.11	4.11	0.11	-1.19	0.05
T (dt4) land-only	0.05	-0.48	0.04	-1.05	0.06	2.10	0.05
	0.1	-0.65	0.04	-1.41	0.05	1.62	0.05
	0.15	-0.53	0.05	-0.68	0.05	1.40	0.05
	0.2	-0.08	0.07	-0.51	0.05	1.22	0.05
T (dt4) mix	0.05	2.50	0.13	3.49	0.11	-0.07	0.05
	0.1	2.22	0.13	3.19	0.11	-0.10	0.03
	0.15	2.18	0.13	2.47	0.11	-0.14	0.04
	0.2	1.95	0.12	2.43	0.10	0.00	0.04
STP (dt4) carbon-only	0.05	52.86	1.31	-86.21	3.86	19.38	1.02
	0.1	52.59	1.31	-86.23	3.87	19.37	1.02
	0.15	52.52	1.32	-86.48	3.87	19.46	1.03
	0.2	52.24	1.32	-86.26	3.87	19.30	1.02
STP (dt4) water-only	0.05	-1.09	0.87	38.27	1.41	-23.27	1.74
	0.1	-1.79	0.93	37.66	1.38	-21.60	1.72
	0.15	-2.58	0.89	37.30	1.42	-21.25	1.69
	0.2	-2.06	0.93	37.11	1.45	-20.60	1.79
STP (dt4) land-only	0.05	-28.82	1.84	12.47	1.87	38.60	0.97
	0.1	-28.16	1.93	11.35	2.01	38.11	1.01
	0.15	-28.63	1.93	12.43	1.94	38.17	1.01
	0.2	-27.82	1.85	11.59	1.84	38.08	1.02
STP (dt4) mix	0.05	2.88	0.46	4.36	0.76	18.20	1.13
	0.1	3.27	0.49	5.09	0.88	16.91	1.17
	0.15	5.33	0.59	3.57	0.85	15.25	1.09
	0.2	0.60	0.56	7.95	1.31	16.76	1.20

Table 11: Scenario 2 - Mix renewable share prediction error sensitivity analysis

- [12] Z. Zhou, F. Liu, R. Zou, J. Liu, H. Xu, H. Jin, Carbon-aware online control of geo-distributed cloud services, *IEEE Transactions on Parallel and Distributed Systems* 27 (9) (2016).
- [13] A. Souza, S. Jatoria, B. Chakrabarty, A. Bridgwater, A. Lundberg, F. Skogh, A. Ali-Eldin, D. Irwin, P. Shenoy, Casper: Carbon-aware scheduling and provisioning for distributed web services, in: *Proceedings of the 14th International Green and Sustainable Computing Conference, IGSC '23*, ACM, 2024.
- [14] T. Sukprasert, A. Souza, N. Bashir, D. Irwin, P. Shenoy, On the limitations of carbon-aware temporal and spatial workload shifting in the cloud, in: *Proceedings of the Nineteenth European Conference on Computer Systems, EuroSys '24*, ACM, 2024.
- [15] R. Cordingly, J. Kaur, D. Dwivedi, W. Lloyd, Towards serverless sky computing: An investigation on global workload distribution to mitigate carbon intensity, network latency, and cost, in: *2023 IEEE International Conference on Cloud Engineering (IC2E)*, 2023.
- [16] L. Lin, A. A. Chien, Adapting datacenter capacity for greener datacenters and grid, in: *Proceedings of the 14th ACM International Conference on Future Energy Systems, e-Energy '23*, ACM, 2023.
- [17] P. Li, J. Yang, M. A. Islam, S. Ren, Making ai less 'thirsty', *Commun. ACM* 68 (7) (2025).
- [18] Y. Jiang, R. B. Roy, R. Kanakagiri, D. Tiwari, Water-wise: Co-optimizing carbon- and water-footprint toward environmentally sustainable cloud computing, in: *Proceedings of the 30th ACM SIGPLAN Annual Symposium on Principles and Practice of Parallel Programming, PPOPP '25*, ACM, 2025.
- [19] T. Newbold, L. N. Hudson, S. L. Hill, S. Contu, I. Lysenko, R. A. Senior, L. Börger, D. J. Bennett, A. Choimes, B. Collen, et al., Global effects of land use on local terrestrial biodiversity, *Nature* 520 (7545) (2015).
- [20] IPCC, *Climate change 2014: Mitigation of climate change. annex iii: Technology-specific cost and performance parameters* (2014).
- [21] J. Macknick, R. Newmark, G. Heath, K. Hallett, *Consumptive water use for u.s. power production* (2011).
- [22] J. Lovering, M. Swain, L. Blomqvist, R. R. Hernandez, Land-use intensity of electricity production and tomorrow's energy landscape, *PLoS One* 17 (7) (2022).
- [23] V. Avelar, D. Azevedo, A. French, E. N. Power, Pue: a comprehensive examination of the metric, *White paper* 49 (2012) 52, accessed: 2026-02-20.
- URL <https://www.thegreengrid.org/en/resources/library-and-tools/20-PUE%3A-A-Comprehensive-Examination-of-the-Metric>
- [24] D. Azevedo, S. C. Belady, J. Pouchet, Water usage effectiveness (wue): A green grid datacenter sustainability metric, *The Green Grid* 32 (2011) 16, accessed: 2026-02-20.
- URL <https://airatwork.com/wp-content/uploads/The-Green-Grid-White-Paper-35-WUE-Usage-Guidelines.pdf>
- [25] K. Sumrani, *Decarbonization: Towards sustainable data centers*, Tech. rep., Dell Technologies, accessed: 2026-02-20 (2023).
- URL [https://learning.dell.com/content/dam/dell-emc/documents/en-us/2023KS\\_Sumrani-Decarbonization\\_To\\_Sustainable\\_Data\\_Centers.pdf](https://learning.dell.com/content/dam/dell-emc/documents/en-us/2023KS_Sumrani-Decarbonization_To_Sustainable_Data_Centers.pdf)
- [26] J. Aslan, K. Mayers, J. G. Koomey, C. France, Electricity intensity of internet data transmission: Untangling the estimates, *Journal of Industrial Ecology* 22 (4) (2018).
- [27] M. Shahradd, R. Fonseca, I. Goiri, G. Chaudhry, P. Batum, J. Cooke, E. Laureano, C. Tresness, M. Russinovich, R. Bianchini, Serverless in the wild: Characterizing and optimizing the serverless workload at a large cloud provider, in: *2020 USENIX annual technical conference (USENIX ATC 20)*, 2020.
- [28] J. Panneerselvam, L. Liu, N. Antonopoulos, Characterisation of hidden periodicity in large-scale cloud datacentre environments, in: *2017 IEEE International Conference on Internet of Things (iThings) and IEEE Green Computing and Communications (GreenCom) and IEEE Cyber, Physical and Social Computing (CPSCom) and IEEE Smart Data (SmartData)*, 2017.
- [29] S. A. Jyothi, C. Curino, I. Menache, S. M. Narayana-murthy, A. Tumanov, J. Yaniv, R. Mavlyutov, I. n. Goiri, S. Krishnan, J. Kulkarni, S. Rao, Morpheus: towards automated slos for enterprise clusters, in: *Proceedings of the 12th USENIX Conference on Operating Systems Design and Implementation, OSDI'16*, USENIX Association, USA, 2016.
- [30] A. Alfadda, R. Adhikari, M. Kuzlu, S. Rahman, Hour-ahead solar pv power forecasting using svr based approach, in: *2017 IEEE Power & Energy Society Innovative Smart Grid Technologies Conference (ISGT)*, IEEE, 2017.
- [31] I. Okumus, A. Dinler, Current status of wind energy forecasting and a hybrid method for hourly predictions, *Energy Conversion and Management* 123 (2016).

- [32] F. Zayas-Gato, A. Díaz-Longueira, P. Arcano-Bea, Á. Michelena, J. L. Calvo-Rolle, E. Jove, A new deep learning-based approach for predicting the geothermal heat pump's thermal power of a real bioclimatic house, *Applied Intelligence* 55 (6) (2025).
- [33] M. Bilgili, S. Keiyinci, F. Ekinici, One-day ahead forecasting of energy production from run-of-river hydroelectric power plants with a deep learning approach, *Scientia Iranica* 29 (4) (2022).
- [34] Our World in Data, What are the safest and cleanest sources of energy?, accessed: 2026-02-20 (2020).  
URL <https://ourworldindata.org/safest-sources-of-energy>
- [35] J. Aslan, K. Mayers, J. G. Koomey, C. France, Electricity intensity of internet data transmission: Untangling the estimates, *Journal of Industrial Ecology* 22 (4) (2018).
- [36] A. D. Popescu, A. Balmin, V. Ercegovac, A. Ailamaki, Predict: towards predicting the runtime of large scale iterative analytics, *Proc. VLDB Endow.* 6 (14) (2013).
- [37] J. Will, L. Thamsen, D. Scheinert, J. Bader, O. Kao, C3o: Collaborative cluster configuration optimization for distributed data processing in public clouds, in: 2021 IEEE International Conference on Cloud Engineering (IC2E), 2021.
- [38] H. Al-Sayeh, B. Memishi, M. A. Jibril, M. Paradies, K.-U. Sattler, Juggler: Autonomous cost optimization and performance prediction of big data applications, in: Proceedings of the 2022 International Conference on Management of Data, SIGMOD '22, Association for Computing Machinery, 2022.
- [39] S. Venkataraman, Z. Yang, M. Franklin, B. Recht, I. Stoica, Ernest: Efficient performance prediction for Large-Scale advanced analytics, in: 13th USENIX Symposium on Networked Systems Design and Implementation (NSDI 16), USENIX Association, 2016.
- [40] D. Weerasiri, M. C. Barukh, B. Benatallah, Q. Z. Sheng, R. Ranjan, A taxonomy and survey of cloud resource orchestration techniques, *ACM Comput. Surv.* 50 (2) (may 2017).
- [41] G. Attenni, N. Bartolini, Environmentally-conscious cloud orchestration considering geo-distributed data centers, Post-Proceedings of the 1st International Workshop on Low Carbon Computing, LOCO '24 (2025).
- [42] M. A. Islam, S. Ren, G. Quan, M. Z. Shakir, A. V. Vasilakos, Water-constrained geographic load balancing in data centers, *IEEE Transactions on Cloud Computing* 5 (2) (2017).
- [43] P. Wiesner, R. Khalili, D. Grinwald, P. Agrawal, L. Thamsen, O. Kao, Fedzero: Leveraging renewable excess energy in federated learning, in: Proceedings of the 15th ACM International Conference on Future and Sustainable Energy Systems, e-Energy '24, ACM, 2024, p. 373–385.
- [44] P. Wiesner, D. Scheinert, T. Wittkopp, L. Thamsen, O. Kao, Cucumber: Renewable-aware admission control for delay-tolerant cloud and edge workloads, in: Euro-Par 2022: Parallel Processing: 28th International Conference on Parallel and Distributed Computing, Springer, 2022, p. 218–232.
- [45] K. West, F. Lehmann, V. Bountris, U. Leser, Y. Elkhatib, L. Thamsen, Exploring the potential of carbon-aware execution for scientific workflows, in: 2025 IEEE 25th International Symposium on Cluster, Cloud and Internet Computing, CCGrid '25, IEEE, 2025, pp. 325–328.

## Appendix A. Other online resources

All the sources were last accessed on the 20th February 2026.

## Appendix B. Azure Data

- for the region swedencentral
  - PUE and WUE values can be found at <https://datacenters.microsoft.com/wp-content/uploads/2024/08/Sweden%2028Sweden%20Central%29.pdf>.
  - The land occupation has been taken from the article "Two municipalities in the Stockholm region sell land to Microsoft", published by Invest Stockholm. Can be accessed at <https://www.mynewsdesk.com/investstockholm/pressreleases/two-municipalities-in-the-stockholm-region-sell-land-to-microsoft-2813124>.
- For the region southcentralus
  - PUE and WUE can be found at <https://datacenters.microsoft.com/wp-content/uploads/2024/08/Texas%2028South%20Central%20US%29.pdf>
  - Land occupation is available at <https://www.datacenters.com/microsoft-azure-south-central-us-texas>.
- For the region centralus
  - PUE and WUE can be found at <https://datacenters.microsoft.com/wp-content/uploads/2024/08/Iowa%2028Central%20US%29.pdf>

- land occupation is available at <https://www.datacenters.com/microsoft-azure-des-moines>.
- For the region eastus2
  - PUE and WUE values can be found at <https://datacenters.microsoft.com/globe/pdfs/sustainability/factsheets/Virginia%20%28East%20US%20&%20East%20US%20%29.pdf>
  - land occupation is available at <https://www.datacenters.com/microsoft-azure-east-us-virginia>.
- FaaS traces can be found in the Azure official GitHub profile. The specific dataset is available at <https://github.com/Azure/AzurePublicDataset/blob/master/AzureFunctionsDataset2019.md>.

## Appendix C. AWS Data

- For all regions
  - PUE and WUE values can be found at <https://sustainability.aboutamazon.com/products-services/aws-cloud>.
  - Land occupation is taken from the FORM 10-K released by Amazon, and is available at [https://s2.q4cdn.com/299287126/files/doc\\_financials/2025/ar/Amazon-2024-Annual-Report.pdf](https://s2.q4cdn.com/299287126/files/doc_financials/2025/ar/Amazon-2024-Annual-Report.pdf).
- Instances memory and cpu can be found at <https://aws.amazon.com/ec2/instance-types>, and bandwidth values at <https://docs.aws.amazon.com/ec2/latest/instancetypes/pg.html>.
- Spark traces are taken from the GitHub repository "scout: A Tool for Cloud Configuration Optimization" available at <https://github.com/oxhead/scout>.

Region	URL
ERCOT	<a href="https://www.eia.gov/electricity/wholesalemarkets/data.php?rto=ercot">https://www.eia.gov/electricity/wholesalemarkets/data.php?rto=ercot</a>
MISO	<a href="https://www.eia.gov/electricity/wholesalemarkets/data.php?rto=miso">https://www.eia.gov/electricity/wholesalemarkets/data.php?rto=miso</a>
PJM	<a href="https://www.eia.gov/electricity/wholesalemarkets/data.php?rto=pjm">https://www.eia.gov/electricity/wholesalemarkets/data.php?rto=pjm</a>
CAISO	<a href="https://www.eia.gov/electricity/wholesalemarkets/data.php?rto=caiso">https://www.eia.gov/electricity/wholesalemarkets/data.php?rto=caiso</a>

Table D.12: US electric grid regions' URLs

## Appendix D. Energy Data

Timeseries of power grid mix.

- *Sweden*: ENTSOE Transparency Platform <https://transparency.entsoe.eu/>,
- *United Kingdom*: National Electricity System Operator API <https://carbon-intensity.github.io/api-definitions/>,
- *Germany*: SMARD - Download market data <https://www.smard.de/en/downloadcenter/download-market-data/>,
- *US*: EIA - Wholesale Electricity Market Data. Table D.12 shows the URLs of the regions that we used in our work.